# CRISPR/Cas9 mutation of a gonad-expressed opsin prevents jellyfish light-induced spawning

**Gonzalo Quiroga Artigas[1], Pascal Lapébie[1], Lucas Leclère[1], Noriyo Takeda[2], Ryusaku Deguchi[3], Gáspár Jékely[4], Tsuyoshi Momose[1]* and Evelyn Houliston[1]***

1. Sorbonne Universités, UPMC Univ. Paris 06, CNRS, Laboratoire de Biologie du Développement de Villefranche-sur-mer (LBDV), 06230 Villefranche-sur-mer, France.

2. Research Center for Marine Biology, Graduate School of Life Sciences, Tohoku University, Asamushi, Aomori, Japan.

3. Department of Biology, Miyagi University of Education, Sendai, Japan

4. Max Planck Institute for Developmental Biology, Spemannstraße 35, 72076 Tübingen, Germany

* corresponding authors

## Abstract

Across the animal kingdom, environmental light cues are widely involved in regulating gamete release, but the molecular and cellular bases of the photoresponsive mechanisms are poorly understood. In hydrozoan jellyfish, spawning is triggered by dark-light or light-dark transitions acting on the gonad, and is mediated by oocyte maturation-inducing neuropeptide hormones (MIHs) released from the gonad ectoderm. Using the model species *Clytia hemisphaerica* we determined that blue-cyan light triggers autonomous spawning in isolated gonads. A candidate opsin (Opsin9) identified from gonad transcriptomes was found co-expressed with MIH within specialised ectodermal neural cells. *Opsin9* knockout jellyfish generated by CRISPR/Cas9 failed to undergo oocyte maturation and spawning, phenotypes reversible by synthetic MIH. We conclude that gamete maturation and release in *Clytia* is regulated by gonadal photosensory-neurosecretory cells that secrete MIH in respose to light via Opsin9. Similar photosensitive-neurosecretory cells in ancestral eumetazoans may have allowed tissue-level photo-regulation of diverse behaviours, a feature elaborated in cnidarians in parallel with expansion of the opsin gene family.

## Introduction

Integration of environmental light information contributes to tight coordination of gamete release in a wide range of animal species. The nature of the photodetection systems involved and their evolutionary origins are poorly undestood. Proposed involvement has mainly focussed on light-entrainment of endogenous clocks, which align many aspects of physiology and behaviour, including reproductive ones, to seasonal, monthly or daily cycles[1,2]. Clock entrainment can involve both of the main

families of photo-sensitive proteins (photopigments) used for animal non-visual photoreception, the evolutionarily ancient Cryptochrome/Photolyase family[3] and the eumetazoan-specific opsin family of light-sensitive G Protein-Coupled Receptors (GPCRs), which are also used for visual photodetection[4]. Light cues can also provide more immediate triggers for gamete release, which integrate with seasonal and/or circadian regulation[5,6], but the involvement of specific photopigments in such regulation has not previously been addressed.

Members of Hydrozoa, a subgroup of Cnidaria which can have jellyfish or polyps as the sexual form[7], commonly display light-regulated sexual reproduction. They have simple gonads in which the germ cells are sandwiched between ectoderm and endoderm, and unlike many other animals lack additional layers of somatic follicle cells surrounding oocytes in the female[8]. Light-dark and/or dark-light transitions trigger the release of mature gametes into the sea water by rupture of the gonad ectoderm[9-11]. Gamete release is coordinated with diel migration behaviours in jellyfish to ensure gamete proximity for fertilisation[12,13]. The photodetection systems that mediate hydrozoan spawning must operate locally within the gonads since isolated gonads will spawn upon dark-light or light-dark transitions[14,15]. Expanded opsin genes families are present in cnidarians and provide good candidates for a role in this process, with expression of some opsin genes reported at the level of the gonad both in the hydrozoan jellyfish *Cladonema radiatum*[16] and in the cubozoan jellyfish *Tripedalia cystophora*[17].

In female hydrozoans, the regulation of spawning is tightly coupled to oocyte maturation, the process by which resting ovarian oocytes resume meiosis to be transformed into fertilisable eggs[18]. Oocyte maturation is induced by “Maturation Inducing hormones” (MIHs), released from gonad somatic tissues upon reception of

the appropriate light cue[14,15]. The molecular identity of MIH of several hydrozoan species has been uncovered as PRPamide family tetrapetides, which are released by scattered neural cells in the gonad ectoderm following dark-light transitions (Takeda et al., submitted; https://doi.org/10.1101/140160). Here we report identification of a cnidarian opsin gene in the hydrozoan jellyfish *Clytia hemisphaerica* and show by gene knockout that it is essential for spawning via MIH release in response to light. We further show that this opsin is expressed in the same gonad ectoderm neural cells that secrete MIH, which thus constitute a key dual function cnidarian cell type responsible for mediating light-induced spawning. These show many features with photosensitive deep brain neuroendocrine cells described in bilaterian species, which may have shared a common origin in ancestral eumetazoans.

## Results

### Spawning *of Clytia* ovaries is induced by blue-cyan light

MIH release in *Clytia* gonads is triggered by a light cue after a minimum dark period of 1-2 hours, with mature eggs being released two hours later[8]. In order to characterise the light response of *Clytia* gonads (Fig.1A), we first assessed the spectral sensitivity of spawning. Groups of 3-6 manually dissected *Clytia* female gonads were cultured overnight in the dark and then stimulated from above with 10-second pulses of monochromatic light across the 340 to 660 nm spectrum. Stimulated ovaries were returned to darkness for one hour before scoring oocyte maturation. Oocyte maturation is accompanied by the breakdown of the oocyte nucleus (Germinal Vesicle) in fully-grown oocytes, followed by spawning. We found that wavelengths between 430 and 520 nm provoked spawning in at least 50% of gonads, with 470-490 nm wavelengths inducing spawning of ≥75% of gonads (Fig.1B). Oocyte maturation and subsequent spawning of *Clytia* of female gonads is thus preferentially triggered by blue-cyan light (Fig.1B), the wavelength range which penetrates seawater the deepest[19,20].

### A highly expressed opsin in *Clytia* gonad ectoderm

We identified a total of ten *Clytia* opsin sequences in transcriptome and genome assemblies from *Clytia* by reciprocal BLAST searches using known hydrozoan opsin sequences[16] and by the presence of the diagnostic lysine in the 7$^{th}$ transmembrane domain to which the retinal chromophore binds[21] (Fig S4). We selected candidate opsins for a role in mediating MIH release by evaluating expression in the isolated gonad ectoderm, which has been shown to have an autonomous capacity to respond to light (Takeda et al., submitted; https://doi.org/10.1101/140160). Illumina HiSeq

reads from gonad ectoderm, gonad endoderm, growing and fully grown oocyte transcriptome sequencing were mapped against each opsin sequence (Fig.2A). In the gonad ectoderm sample, two opsin mRNAs (*Opsin4* and *Opsin7*) were detected at low levels and one was very highly expressed (*Opsin9*), while in the three other analysed gonad samples opsin expression was virtually undetectable (Fig.2A). The high expression of *Opsin9* gene in the gonad ectoderm made it a strong candidate for involvement in light-induced spawning.

Molecular phylogenies constructed from an alignment of the 10 *Clytia* opsin amino acid sequences and published dataset comprising a comprehensive subset of eumetazoan opsins[22] positioned all *Clytia* opsins within a clade containing only opsins from medusozoan cnidarians (Fig.S1). The picture of expansion of the opsin gene family within the Medusozoa was reinforced by more detailed analysis of all hydrozoan and cubozoan opsin sequences available in GenBank, *Clytia* Opsin9 (along with the closely related Opsin10) being amongst the most divergent sequences (Fig. S2, S3). Additional evidence for a distinct evolutionary history for these sequences came from analysis of draft genome sequences (not shown) revealing that *Clytia Opsin9* and *Opsin10*, unlike all other described medusozoan opsin genes[17], contain an intron in a distinct position to the one predicted for the ancestral eumetazoan opsin. We confirmed, however, that the Opsin9 amino acid sequence exhibits all the hallmarks of a functional photopigment (Fig.S4), with conserved amino acids at positions required for critical disulphide bond formation and for Schiff base linkage to the retinal chromophore[4,23,24], including acidic residues at the both potential ‘counterion’ positions, only one of which is largely conserved in cnidarian opsin sequences[17]. The Glu/Asp-Arg-Tyr/Phe motif adjacent to the third

transmembrane domain, involved in cytoplasmic signal transduction via G proteins[23-25] is also present in Opsin9.

Opsin sequence evolution is rapid and the exact relationship of Opsin9/10 and other medusozoan opsins cannot be resolved with the available data, due to low branch support values, probable long-branch attraction effects, the variable topologies of Maximum Likelihood (ML) (Fig.S2) and Bayesian (Fig.S3) trees and unstable position of Opsin9/10 under different choices of evolutionary model (not shown). ML and Bayesian phylogenies and AU ("approximately unbiased") phylogenetic tests[26] unambiguously showed, however, that *Clytia Opsin9* is not orthologous to gonad-expressed opsin genes identified in *Cladonema* (AU test: $p < 1e-4$) or in *Tripedelia* (AU test: $p < 1e-8$). Thus the expression of any particular opsin genes in the gonad is unlikely to be a common ancestral feature of the medusozoans.

### *Opsin9* is expressed in MIH-secreting gonad ectoderm cells

In situ hybridisation of *Clytia* ovaries revealed *Opsin9* expression in a scattered population of gonad ectoderm cells (Fig.2B), but not anywhere else in the jellyfish (not shown). We were unable to detect by in situ hybridisation in *Clytia* gonads either of the two lowly-expressed gonad ectoderm opsin genes, *Opsin4* and *Opsin7* (Fig.2D-E). The distribution of *Opsin9*-expressing cells was highly reminiscent of the expression pattern for *PP1* and *PP4* (Fig.2C), the two MIH neuropeptide precursor genes co-expressed in a common gonad ectoderm neural population (Takeda et al., submitted; https://doi.org/10.1101/140160). Double fluorescent in situ hybridisation using probes for *Opsin9* and for *PP4* revealed that these genes were expressed in the same cells (Fig.2F); 99% of Opsin9 mRNA positive cells were also positive for PP4 mRNA, and over 87% of *PP4 mRNA*-positive cells were also positive for *Opsin9*

mRNA. This finding raised the possibility that spawning in *Clytia* might be directly controlled by light detection through an opsin photopigment in the MIH-neurosecretory cells of the gonad ectoderm.

### *Opsin9* gene knockout prevents oocyte maturation and spawning

To test the function of Opsin9 in light-induced oocyte maturation and spawning, we generated a *Clytia Opsin9* knockout (KO) polyp colony using a CRISPR/Cas9 approach, which produces very extensive bi-allelic KO of the targeted gene in the F0 generation[27] (see methods for details). This approach is favoured by the *Clytia* life cycle, in which larvae developed from each CRISPR-injected egg metamorphose into a vegetatively-expanding polyp colony, from which sexual jellyfish stage bud clonally[7,28]. CRISPR guide RNAs were designed to target a site in the first exon of *Opsin9* encoding the 3$^{rd}$ transmembrane domain, and were verified not to match any other sites in available genome sequences. One of the polyp colonies generated carried a predominant 5-bp deletion, corresponding to a frame-shift and premature STOP codon (Fig.3A). Polyp colony development in this individual, *Opsin9*$^{n1–4}$, showed no abnormal features.

For phenotypic analysis we collected *Opsin9*$^{n1–4}$ jellyfish, which were all females, and grew them by twice-daily feeding for two weeks to sexual maturity. Although these *Opsin9*$^{n1–4}$ mature medusae initially appeared normal, they did not spawn after the daily dark-light transition, and after a few days displayed grossly inflated ovaries due to an accumulation of unreleased immature oocytes (Fig.3B-C). In three independent experiments to test the light response of isolated gonads, over 85% of *Opsin9* KO gonads failed to undergo oocyte maturation and spawning upon light stimulation (Fig.3D).

Genotyping of individual gonads showed that the rare gonads from *Opsin9*$^{n1\_4}$ medusae that spawned after light had greater mosaicism of mutations, with a higher ratio of residual non-frameshift mutations and also a significant amount of wild type cells, whereas gonads that failed to spawn carried mainly the predominant 5-bp deletion, a second 21-bp deletion and no wild type cells (Fig.S5).

The failure of spawning observed in *Clytia* Opsin9 KO mutant jellyfish gonads, together with the absence of detectable Opsin9 expression in non-gonad tissues of the medusa and the autonomous response of isolated wild-type gonads to light, strongly indicates that the gonad photopigment Opsin9 plays an essential role in light-induced oocyte maturation.

**Opsin9 is required for light-induced MIH secretion from gonad ectoderm**

Since Opsin9 and MIH are co-expressed in the same cells, we reasoned that *Opsin9* function was probably required for MIH secretion. Two experimental approaches confirmed this hypothesis. Firstly, treatment of *Opsin9* mutant gonads with synthetic MIH peptides was able to rescue fully the mutant phenotype. Equivalent MIH concentrations to those effective for light-adapted isolated gonads (Takeda et al., submitted; https://doi.org/10.1101/140160) reliably induced oocyte maturation and spawning in *Opsin9* KO isolated gonads (Fig. 3E). Spawned eggs from *Opsin9* mutants could be fertilised and to develop into larvae, although the fertilisation rate was lower than for oocytes spawned in parallel from wild type gonads (not shown). Secondly, we showed by immunofluorescence that MIH release was compromised in *Opsin9* mutant gonads (Fig. 4). Quantitative immunofluorescence analyses based on anti-MIH staining and fluorescence levels were performed in both wild type and *Opsin9* mutant gonads, comparing light-adapted and dark-adapted specimens fixed

45 minutes after white light exposure. Whereas wild type gonads exhibited a significant decrease of MIH fluorescence values in MIH-secreting neural cells upon light stimulation (Fig. 4A-C), *Opsin9* mutant gonads maintained similar levels of MIH fluorescence in both conditions (Fig.4D-F). Moreover, average MIH fluorescence levels per cell were significantly higher (U test: $p < 0.001$), in *Opsin9* mutant than in wild type ovaries suggesting a progressive accumulation of MIH in *Opsin9* mutant gonads.

Taken together, these results demonstrate that Opsin9 is required for MIH-neurosecretory cells in the *Clytia* gonad to release MIH following dark-light transitions, and thus has an essential role in light-dependent reproductive control.

**Neuronal morphology of *Clytia* gonad MIH-secreting cells**

The functional studies described above indicate that *Clytia* gonad cells that co-express MIH and Opsin9 have a photosensory functions, as well as a neurosecretory characteristics (Takeda et al, submitted; https://doi.org/10.1101/140160). To investigate the morphology of these key cells in more detail we performed immunofluorescence to visualise microtubules and cortical actin in cells producing MIH (Fig.5). The *Clytia* gonad ectoderm consists of a monolayer of ciliated epitheliomuscular cells[29], tightly coupled by apical junctions, and bearing basal extensions containing muscle fibres, which form a layer over the oocytes (Fig.5A-C, E-F). The MIH-secreting neural cells were found to be scattered among epitheliomuscular cells and to be much less abundant (Fig.5D, G). A variable number of neural processes (Fig.5D, G) project basally from these cells, and intermingle with the muscle fibres of surrounding epitheliomuscular cells (Fig.5F), but did not appear to form a connected network (Fig.5G). The cell nuclei were generally located more

basally than those of the surrounding epitheliomuscular cells (Fig.5F-F'). In some cases we could detect small apical domains of MIH-positive cells at the epithelium surfaces associated with basal bodies and cilia (Fig.5D, H-H'). The presence of gaps separating the gonad ectoderm and the large oocytes (Fig5.C, E), probably containing extracellular jelly components produced during late stages of oocyte growth, suggests that the peptide hormone (MIH) is probably secreted at a distance from its site of action at the oocyte surface.

These immunofluorescence analyses indicate that the MIH-secreting cells have morphological features characteristic of multipolar neurosensory cells in cnidarians[30]. Based on gene expression, morphology and biological function we propose that this cell type has a dual sensory-neurosecretory nature.

To summarise the results of this study, we have provided the first demonstration, using CRISPR/Cas9–mediated gene knockout, of an essential role for an opsin gene in non-visual photodetection in a cnidarian. *Clytia* Opsin9 is required for a direct light-response mechanism that acts locally in the gonad to trigger gamete maturation and release (Fig. 6). It acts in specialised sensory-neurosecretory cells of the *Clytia* gonad ectoderm to trigger MIH secretion from these cells upon light reception. This peptidic MIH in turn induces oocyte maturation in females, and also release of motile sperm in males (Takeda et al., submitted; https://doi.org/10.1101/140160), efficiently synchronising spawning to maximise reproductive success.

## Discussion

Comparison of neuropeptide involvement in hydrozoan, starfish, fish and frog reproduction suggested an evolutionary scenario in which gamete maturation and release in ancient metazoans was triggered by gonad neurosecretory cells (Takeda et al, submitted; https://doi.org/10.1101/140160). According to this scenario, this cell type would have been largely conserved during cnidarian evolution and function similarly today in hydrozoans, whereas during bilaterian evolution further levels of regulation were inserted between the secreting neurons and the responding gametes, such that peptide hormone secretion in vertebrates was delocalised to the hypothalamus, and the primary responding cells to the pituitary. Our study on opsins has further revealed a parallel between the MIH-secreting cells of the gonad ectoderm in *Clytia* and deep brain photoreceptor cells in vertebrates, as well as equivalent cells in various protostome species that regulate physiological responses through neurohormone release in response to ambient light[31-34]. Like the *Clytia* MIH-producing cells, TSH-producing cells in birds and fish pituitary[35,36], and vasopressin/oxytocin-expressing cells in fish hypothalamus and annelid forebrain[34], show opsin-related photodetection, secrete neuropeptide hormones and are implicated in hormonal control of reproduction[37]. We can thus propose that the putative neurosecretory cell type associated with the germ line that regulated gamete release in ancestral metazoans was also photosensitive. The active photopigments in these cells could have been cryptochromes, the most ancient metazoan photopigment family inherited from unicellular ancestors and apparently used exclusively in sponges[4,38] or animal opsins, whose gene family expanded extensively in both cnidarians and bilaterians from an ancestral eumetazoan GPCR gene[4,17,22,39]. Under this evolutionary scenario, the essential Opsin9 protein in *Clytia*, and similarly

the gonad-expressed *Cladonema*[16] and *Tripedalia*[17] opsins, would have replaced the ancestral photopigment in the MIH-secreting cells during cnidarian evolution to provide optimised spawning responses to particular light wavelength and intensity. A parallel can be drawn with the evolution of vision in eumetazoans, in which deployment of animal opsins is thought to have allowed more rapid and precise photoresponses than the ancestral cryptochrome system[4].

While the scenario above conforms to the evolutionary trend for specialised cell types with distributed functions in bilaterians to evolve from ancestral multifunctional cell types[40,41], an alternative hypothesis is that the *Clytia* gonad photosensitive–neurosecretory cells and bilaterian deep brain photoreceptors arose convergently during evolution. Specifically, a population of MIH-secreting cells in hydrozoan gonads, initially regulated by other environmental and/or neural inputs, may have secondarily acquired opsin expression to become directly photosensitive. More widely, cnidarians may have accumulated a variety of multifunctional cell types as specific populations of neural cells, muscle cells or nematocytes acquired photopigments during evolution[42]. Cnidarians are characterised by the lack of a centralised nervous system, and correspondingly show localised regulation of many physiological processes and behaviours at the organ, tissue or even the cellular levels. In addition to gamete release, other local light-mediated responses include light-sensitive discharge of cnidocyte-associated sensory-motor neurons expressing hydra *HmOps2*[43], diel cycles of swimming activity[12,13] controlled in *Polyorchis* by photoresponsive cells of the inner nerve ring[44], and tentacle retraction in corals[45]. *Clytia* Opsin9, the first cnidarian opsin to have a demonstrated function, is expressed in the scattered, MIH-secreting cells, which act autonomously in the gonad and

appear to respond individually to light with no obvious coordination of MIH release between them (see Fig. 4, 5G).

Whether Hydrozoa gonad ectoderm MIH-secreting cells and Bilateria deep brain photosensitive cells derived from an ancestral multifunctional sensory-neurosecretory cell type, or from non-photoresponsive neuronal cells remains an open question. Our findings support a scenario in which expansion of the opsin gene family within the hydrozoan clade was accompanied by the local deployment of individual opsins with specific spectral characteristics adjusted to regulate a variety of physiological behaviours in response to light, epitomised by *Clytia* Opsin9 and its regulation of spawning.

# Methods

### *Animals*

Sexually mature medusae from laboratory maintained *Clytia hemisphaerica* ("Z colonies") were fed regularly with *Artemia* nauplii and cultured under light-dark cycles to allow daily spawning. Red Sea Salt brand artificial seawater (ASW) was used for all culture and experiments.

### *Monochromator assay*

Manually dissected *Clytia* ovaries in small plastic petri dishes containing Millipore filtered sea water (MFSW) were maintained overnight in the dark and then stimulated with monochromatic light, provided by a monochromator (PolyChrome II, Till Photonics) installed above the samples, using the set-up described by Gühmann et al.,[20], which delivers equivalent levels of irradiance between 400 and 600 nm (3.2E+18 to 4.3E+18 photons/s/m2). Monochromatic light excitation was carried out

in a dark room. 10 second pulses of different wavelengths, between 340 to 660 nm were applied to separate groups of 3-6 gonads, which were then returned to darkness for one hour before monitoring of oocyte maturation seen as loss of the oocyte nucleus (Germinal Vesicle) in fully grown oocytes, followed by spawning. A wavelength was acknowledged to induce maturation if at least one oocyte per gonad underwent maturation and spawning within the correct timing[45] after monochromatic light excitation. 10-second exposure times were chosen because initial trials (not shown) showed that these gave sub-saturating responses at all wavelengths. Gonads that spawned prematurely due to manipulation stress were excluded from analysis.

### *Identification of Clytia opsin genes*

BLAST searches were performed on an assembled *Clytia hemisphaerica* mixed-stage transcriptome containing 86,606 contigs, using published cnidarian opsin sequences or *Clytia* opsin sequences as bait. The ORFs of selected *Clytia* opsins were cloned by PCR into pGEM-T easy vector for synthesis of in situ hybridisation probes. Sequences and accession numbers for the opsin sequences analysed in this study are given in File S1.

### *Gonad transcriptome analysis*

Illlumina HiSeq 50nt reads were generated from mRNA isolated using RNAqueous micro kit (Ambion Life technologies, CA) from ectoderm, endoderm, growing oocytes and fully grown oocytes manually dissected from about 150 *Clytia* female gonads. The reads were mapped against the opsin sequences retrieved from a *Clytia* reference transcriptome using Bowtie2[46]. The counts for each contig were normalised per total of reads of each sample and per sequence length. Opsins RNA read counts

from each tissue were visualised as a colour coded heat map using ImageJ software.

### *Opsin molecular phylogeny*

To assess the relationship of the *Clytia* opsin amino acid sequences to known opsins, they were added to the Feuda et al., (2014)[22] dataset using the profile alignment option in MUSCLE[47] with Seaview v4.2.12[48]. The alignment was manually trimmed to remove positions only present in the newly added *Clytia* opsin sequences. A subset of this alignment was highlighted by similarity group conservation (defined by GeneDoc and the BLOSUM62 matrix – FigS4). For more detailed comparison between medusozoan sequences, all cubozoan and hydrozoan currently available opsin protein sequences in GenBank were retrieved from NCBI and added to the 10 *Clytia* opsin sequences. Cd-hit[49] was run with 99% identity to eliminate sequence duplicates, obtaining a final dataset of 56 Cubozoa and Hydrozoa opsin protein sequences (FASTA file available in File S4). The alignment was performed using the MUSCLE algorithm with MEGA7[50], and was further adjusted manually to remove sites at the 3'- and 5'-ends as well as regions where gaps were created by one individual sequence. The trimmed alignments are in Files S2 and S3 (phylip interleaved format).

Both alignments (Feuda et al., 2014 + *Clytia* opsins, and Hydrozoa + Cubozoa opsins) were subjected to Maximum likelihood (ML) and Bayesian analyses using RaxML GUI1.5b[51] and MrBayes 3.2.6[52] respectively. The GTR+G model of protein evolution was used, since it provides a better fit for opsin sequences than other models[39]. Support for the branches in the ML phylogenies was estimated using non-parametric bootstrapping (500 replicates). Bayesian analyses were subjected to 2 independent runs of four chains, temp = 0.2 and 10000000 generations. Both

datasets analyses were considered to have converged since average standard deviation of split frequencies dropped below 0.05. Consensus trees and posterior probabilities were calculated once the stationary phase was obtained. A ML tree was used as a starting guide tree for the Feuda et al., (2014) + *Clytia* opsins alignment. Melatonin receptors for the bilaterian + cnidarian + ctenophore tree were chosen as the outgroup for opsin phylogeny[39]. The resulting trees were visualised with FigTree (http://tree.bio.ed.ac.uk/software/figtree/).

Approximated Unbiased (AU) phylogenetic tests[26] were performed as described previously[53]. Values presented in the result section were obtained comparing, among others, the ML tree with *Clytia* Opsin9, Opsin10 and either *Cladonema* or *Tripedalia* gonad-expressed Opsins constrained as monophyletic using RaxML. Exclusion of the non-gonad-expressed Opsin10 from these monophyletic constraints led to much lower p values (not shown).

### *In situ hybridisation*

For *in situ* hybridization, isolated gonads were processed as previously[54] except that 4M Urea was used instead of 50% formamide in the hybridization buffer as it significantly improves signal detection and sample preservation in *Clytia* medusae[55]. Images were taken with an Olympus BX51 light microscope. For double fluorescent *in situ* hybridisation, female *Clytia* gonads were fixed overnight at 18ºC in HEM buffer (0.1 M HEPES pH 6.9, 50 mM EGTA, 10 mM $MgSO_4$) containing 3.7% formaldehyde, washed five times in PBS containing 0.1% Tween20 (PBS-T), then dehydrated on ice using 50% methanol/PBS-T then 100% methanol. *In situ* hybridisation was performed using a DIG-labeled probe for Opsin9 and a fluorescein-labeled probe for PP4. A three hours incubation with a peroxidase-labeled anti-DIG antibody was followed by

washes in MABT (100 mM maleic acid pH 7.5, 150 mM NaCl, 0.1% Triton X-100). For Opsin9 the fluorescence signal was developed using the TSA (Tyramide Signal Amplification) kit (TSA Plus Fluorescence Amplification kit, PerkinElmer, Waltham, MA) and Cy5 fluorophore (diluted 1/400 in TSA buffer: PBS/$H_2O_2$ 0.0015%) at room temperature for 30 min. After 3 washes in PBS-T, fluorescence was quenched with 0.01N HCl for 10 min at room temperature and washed again several times in PBS-T. Overnight incubation with a peroxidase-labelled anti-fluorescein antibody was followed by washes in MABT. The anti PP4 fluorescence signal was developed using TSA kit with Cy3 fluorophore. Controls with single probes were done to guarantee a correct fluorescence quenching and ensure that the two channels did not cross-react. Nuclei were stained using Hoechst dye 33258. Images were acquired using a Leica SP5 confocal microscope and maximum intensity projections of z-stacks prepared using ImageJ software.

***Immunofluorescence***

For co-staining of neuropeptides and tyrosinated tubulin, dissected *Clytia* gonads were fixed overnight at 18ºC in HEM buffer containing 3.7% formaldehyde, then washed five times in PBS containing 0.1% Tween20 (PBS-T). Treatment on ice with 50% methanol/PBS-T then 100% methanol plus storage in methanol at -20ºC improved visualisation of microtubules in the MIH-producing cells. Samples were rehydrated, washed several times in PBS-0.02% Triton X-100, then one time in PBS-0.2% Triton X-100 for 20 minutes, and again several times in PBS-0.02% Triton X-100. They were then blocked in PBS with 3% BSA overnight at 4ºC. The day after they were incubated in anti-PRPamide antibody and anti-Tyr tubulin (YL1/2, Thermo Fisher Scientific) in PBS/BSA at room temperature for 2 h. After washes, the

specimens were incubated with secondary antibodies (Rhodamine goat anti-rabbit and Cy5 donkey anti-rat-IgG; Jackson ImmunoResearch, West Grove, PA) overnight in PBS at 4ºC, and nuclei stained using Hoechst dye 33258 for 20 min.

For co-staining of neuropeptides with cortical actin or ɣ-Tubulin, dissected *Clytia* gonads were fixed for 2-3 hours at room temperature in HEM buffer containing 80mM maltose, 0.2% Triton X-100 and 4% paraformaldehyde, then washed five times in PBS containing 0.1% Tween20 (PBS-T). Samples were further washed in PBS-0.02% Triton X-100, then one time in PBS-0.2% Triton X-100 for 20 minutes, and again several times in PBS-0.02% Triton X-100. They were then blocked in PBS with 3% BSA overnight at 4ºC. The day after they were incubated in anti-PRPamide antibody and anti- ɣ-Tubulin (GTU-88, Sigma Aldrich), or only anti-PRPamide, in PBS/BSA at room temperature for 2 h. After washes, the specimens were incubated with secondary antibodies (Rhodamine goat anti-rabbit and Cy5 goat anti-mouse-IgG) or Phalloidin-Rhodamine and secondary antibody (Cy5 goat anti-rabbit) overnight in PBS at 4ºC, and nuclei stained using Hoechst dye 33258 for 20 min. Images were acquired using a Leica SP8 confocal microscope and maximum intensity projections of z-stacks prepared using ImageJ software.

For MIH fluorescence quantification, 5-6 independent gonads for each of the two conditions (light-adapted and dark-adapted after light stimulation) and *Clytia* strains (WT and *Opsin9*$^{n1-4}$) were fixed as mentioned above and co-stained for MIH and Tyr-tubulin. All the fixations were done in parallel. Confocal images were acquired using the same scanning parameters (i.e. magnification, laser intensity and gain). In all cases, 10 confocal Z planes were summed over 4 µm depth at the gonad surface using ImageJ software. With ImageJ, we separated the two channels (MIH and Tyr-tubulin) and selected the contour of MIH-positive cells using the Tyr-tubulin staining

as guidance. Using the “Integrated Density” option, we recovered the “RawIntDen” values of the MIH-stained channel, which refer to the sum of the pixel intensity values in the selected region of interest. These values divided by 1000 correspond to the RFU (Relative Fluorescence Units) in Figure 4.

### *Generation of CRISPR-Cas9 mutant Clytia colonies*

The template for *Opsin9* n1 small guide RNA (sgRNA) was assembled by cloning annealed oligonucleotides corresponding 20 bp Opsin9 target sequence into pDR274[56] (42250, Addgene), which contains tracrRNA sequence next to a BsaI oligonucleotide insertion site. The sgRNA was then synthesised from the linearised plasmid using Megashortscript T7 kit (Thermo Fisher Scientific) and purified with ProbeQuant G-50 column (GE healthcare) and ethanol precipitation. sgRNA was dissolved in distilled water at 80 µM and kept at -80ºC until use. The *opsin9* n1 sequence is shown in FileS5. Purified Cas9 protein dissolved in Cas9 buffer (10 mM Hepes, 150 mM KCl) was kindly provided by J-P Concordet (MNHN Paris) and diluted to 5 µM. sgRNA was added to Cas9 protein in excess (2:1) prior to injection and incubated for 10 minutes at room temperature. The final Cas9 concentration was adjusted to 4.5 µM and the sgRNA to 9 µM. The mixture was centrifuged at 14,000 rpm for 10 minutes at room temperature. 2-3% of egg volume was injected into unfertilised eggs within 1 hour after spawning, prior to fertilisation.

Injected embryos were cultured for 3 days in MFSW at 18°C. Metamorphosis of planula larvae into polyps was induced about 72 hours after fertilisation by placing larvae (20-80/slide) on double-width glass slides (75 x 50mm) in drops of 3-4ml MFSW containing 1 µg/ml synthetic metamorphosis peptide (GNPPGLW-amide), followed by overnight incubation. Slides with fixed primary polyps were transferred to

small aquariums kept at 24°C, to favour the establishment of female colonies[57]. Primary polyps and young polyp colonies were fed twice a day with smashed *Artemia* nauplii until they were grown enough to be fed with swimming nauplii. Following colony vegetative expansion, a single well-growing colony on each slide was maintained as a founder. After several weeks of growth, polyp colonies were genotyped to assess mutation efficiency and mosaicism, and medusae were collected from the most strongly mutant colony (*Opsin9*$^{n1-4}$) for further experimentation.

### *Mutant genotyping*

Genomic DNA from *Clytia* polyps and jellyfish gonads was purified using DNeasy blood/tissue extraction kit (Qiagen). The *opsin9* target site was amplified by PCR using Phusion DNA polymerase (New England Biolabs). Primers used for genotyping are listed in FileS5. PCR products were sequenced and mutation efficiency was assessed using TIDE analyses (Fig.S5), which estimates the mutation composition from a heterogeneous PCR product in comparison to a wild type sequence[58].
We scanned *Clytia* genome for possible off-targets of *Opsin9* sgRNA at http://crispor.tefor.net. From 2 possible off-targets where Cas9 could cut, none was found in coding sequences nor were they right next to a PAM sequence.

### *Gonad spawning assays*

Sexually mature wild type and *opsin9*$^{n1-4}$ mutant medusae of the same age and adapted to the same day-night cycle were collected for gonad dissection. Individual gonads were transferred to 100µl MFSW in 96-well plastic plates. Plates were covered with aluminium foil overnight and brought back to white light the following

day. For the rescue experiment with synthetic MIH, wild type and *opsin9*$^{n1-4}$ mutant gonads adapted to light conditions were dissected and transferred to 96-well plastic plates and acclimatised for two hours. 100µl of a stock of 2x10-7M synthetic WPRPamide (synthetic MIH) in MFSW was added in each well to give a final concentration of 10-7M. Oocyte maturation was scored after one hour. Spawning followed in all cases where oocyte maturation was triggered. Gonads that spawned prematurely due to manipulation stress were excluded from analysis. Gonad pictures in Fig.3 were taken with an Olympus BX51 microscope.

### *Graphs and statistics*

Graphs and statistics for the monochromator assay were prepared using BoxPlotR[59]. Fisher exact tests and Mann-Whitney U tests were performed at http://www.socscistatistics.com. Mann-Whitney U tests were chosen for MIH fluorescence quantification comparisons since the results did not follow a normal distribution following Shapiro-Wilk test.

## Acknowledgements

We thank M. Khamla for the graphics in Figure 1, J-P Concordet (MNHN Paris) for generously providing Cas9 protein, M. Gühmann for monochromator training, and all our laboratory and NEPTUNE colleagues for stimulating and critical discussions.

Funding was provided by the Marie Curie ITN NEPTUNE, French ANR grant OOCAMP and core CNRS funding to the LBDV.

# REFERENCES

1. Cermakian, N. & Sassone-Corsi, P. Environmental stimulus perception and control of circadian clocks. *Curr. Opin. Neurobiol.* **12,** 359–365 (2002).
2. Tessmar-Raible, K., Raible, F. & Arboleda, E. Another place, another timer: Marine species and the rhythms of life. *Bioessays* **33,** 165–172 (2011).
3. Oliveri, P. *et al.* The Cryptochrome/Photolyase Family in aquatic organisms. *Mar Genomics* **14,** 23–37 (2014).
4. Gehring, W. J. The evolution of vision. *WIREs Dev Biol* **3,** 1–40 (2014).
5. Lambert, C. C. & Brandt, C. L. The effect of light on the spawning of Ciona intestinalis. *Biol. Bull.* **132,** 222–228 (1967).
6. Kaniewska, P. *et al.* Signaling cascades and the importance of moonlight in coral broadcast mass spawning. *Elife* **4,** e09991 (2015).
7. Leclère, L., Copley, R. R., Momose, T. & Houliston, E. Hydrozoan insights in animal development and evolution. *Current Opinion in Genetics & Development* **39,** 157–167 (2016).
8. Deguchi, R., Takeda, N. & Stricker, S. A. Comparative biology of cAMP-induced germinal vesicle breakdown in marine invertebrate oocytes. *Mol. Reprod. Dev.* **78,** 708–725 (2011).
9. Miller, R. L. Sperm chemotaxis in the hydromedusae. I. Species-specificity and sperm behavior. *Marine Biology* **53,** 99–113 (1979).
10. Roosen-Runge, E. C. On the biology of sexual reproduction of hydromedusae, genus *Phialidium Leuckhart*. *Pacif Sci* **XVI,** 15–24 (1962).
11. Freeman, G. & Ridgway, E. B. The role of cAMP in oocyte maturation and the role of the germinal vesicle contents in mediating maturation and subsequent

developmental events in hydrozoans. *Dev. Genes Evol.* **197,** 197–211 (1988).

12. Mills, C. E. Vertical migration and diel activity patterns of hydromedusae: studies in a large tank. *J Plankton Res* **5,** 619–635 (1983).
13. Martin, V. J. Photoreceptors of cnidarians. **80,** 1703–1722 (2011).
14. Ikegami, S., Honji, N. & Yoshida, M. Light-controlled production of spawning-inducing substance in jellyfish ovary. *Nature* **272,** 611–612 (1987).
15. Freeman, G. The role of oocyte maturation in the ontogeny of the fertilization site in the hydrozoan *Hydractinia echinata*. *Roux's Arch Dev Biol* **196,** 83–92 (1987).
16. Suga, H., Schmid, V. & Gehring, W. J. Evolution and functional diversity of jellyfish Opsins. *Current Biology* **18,** 51–55 (2008).
17. Liegertová, M. *et al.* Cubozoan genome illuminates functional diversification of opsins and photoreceptor evolution. *Sci Rep* **5,** 11885 (2015).
18. Yamashita, M., Mita, K., Yoshida, N. & Kondo, T. Molecular mechanisms of the initiation of oocyte maturation: general and species-specific aspects. *Prog Cell Cycle Res* **4,** 115–129 (2000).
19. Gehring, W. & Rosbash, M. The coevolution of blue-light photoreception and circadian rhythms. *J. Mol. Evol.* **57,** S286–S289 (2003).
20. Guehmann, M. *et al.* Spectral tuning of phototaxis by a Go-Opsin in the rhabdomeric eyes of *Platynereis*. *Current Biology* **25,** 2265–2271 (2015).
21. Terakita, A., Kawano-Yamashita, E. & Koyanagi, M. Evolution and diversity of opsins. *WIREs Membr Transp Signal* **1,** 104–111 (2011).
22. Feuda, R., Rota-Stabelli, O., Oakley, T. H. & Pisani, D. The comb jelly opsins and the origins of animal phototransduction. *Genome Biol. Evol.***6,** 1964–1971 (2014).

23. Schnitzler, C. E. *et al.* Genomic organization, evolution, and expression of photoprotein and opsin genes in *Mnemiopsis leidyi:* a new view of ctenophore photocytes. *BMC Biol.* **10,** 107 (2012).

24. Fischer, R. M. *et al.* Co-expression of VAL- and TMT-opsins uncovers ancient photosensory interneurons and motorneurons in the vertebrate brain. *PLoS Biol.* **11,** e1001585 (2013).

25. Kojima, D., Mano, H. & Fukada, Y. Vertebrate ancient-long opsin: a green-sensitive photoreceptive molecule present in zebrafish deep brain and retinal horizontal cells. *J. Neurosci.* **20,** 2845–2851 (2000).

26. Shimodaira, H. An approximately unbiased test of phylogenetic tree selection. *Systematic Biology* **51,** 492–508 (2002).

27. Momose, T. & Concordet, J.-P. Diving into marine genomics with CRISPR/Cas9 systems. *Mar Genomics* **30,** 55–65 (2016).

28. Houliston, E., Momose, T. & Manuel, M. *Clytia hemisphaerica*: a jellyfish cousin joins the laboratory. *Trends Genet.* **26,** 159–167 (2010).

29. Leclère, L. & Röttinger, E. Diversity of cnidarian muscles: Function, anatomy, development and regeneration. *Front. Cell Dev. Biol.* **4,** E3365–22 (2017).

30. Saripalli, L. D. & Westfall, J. A. Classification of nerve cells dissociated from tentacles of the sea anemone *Calliactis parasitica*. *Biol. Bull.* **190,** 111–124 (1996).

31. Fernandes, A. M., Fero, K., Driever, W. & Burgess, H. A. Enlightening the brain: linking deep brain photoreception with behavior and physiology. *Bioessays* **35,** 775–779 (2013).

32. Fischer, R. M. *et al.* Co-expression of VAL- and TMT-Opsins uncovers ancient photosensory interneurons and motorneurons in the vertebrate brain. *PLoS*

*Biol.* **11,** e1001585–16 (2013).

33. Halford, S. *et al.* VA opsin-based photoreceptors in the hypothalamus of birds. *Curr. Biol.* **19,** 1396–1402 (2009).
34. Tessmar-Raible, K. *et al.* Conserved sensory-neurosecretory cell types in annelid and fish forebrain: insights into hypothalamus evolution. *Cell* **129,** 1389–1400 (2007).
35. Vigh, B. *et al.* Nonvisual photoreceptors of the deep brain, pineal organs and retina. *Histol. Histopathol.* **17,** 555–590 (2002).
36. Nakane, Y. *et al.* The saccus vasculosus of fish is a sensor of seasonal changes in day length. *Nature Communications* **4,** 2108 (2013).
37. Juntti, S. A. & Fernald, R. D. Timing reproduction in teleost fish: cues and mechanisms. *Curr. Opin. Neurobiol.* **38,** 57–62 (2016).
38. Cronin, T. W. & Porter, M. L. The Evolution of Invertebrate Photopigments and Photoreceptors in *Evolution of Visual and Non-visual Pigments* ed T.M. Hunt *et al. Springer US*, 105–135 (2014).
39. Feuda, R., Hamilton, S. C., McInerney, J. O. & Pisani, D. Metazoan opsin evolution reveals a simple route to animal vision. *Proc. Natl. Acad. Sci. U.S.A.* **109,** 18868–18872 (2012).
40. Arendt, D. The evolution of cell types in animals: emerging principles from molecular studies. *Nat Rev Genet* **9,** 868–882 (2008).
41. Arendt, D. *et al.* The origin and evolution of cell types. *Nat Rev Genet* **17,** 744–757 (2016).
42. Porter, M. L. *et al.* Shedding new light on opsin evolution. *Proceedings of the Royal Society B: Biological Sciences* **279,** 3–14 (2012).
43. Plachetzki, D. C., Fong, C. R. & Oakley, T. H. Cnidocyte discharge is regulated

by light and opsin-mediated phototransduction. *BMC Biol.* **10,** 17 (2012).

44. Anderson, P. A. & Mackie, G. O. Electrically coupled, photosensitive neurons control swimming in a jellyfish. *Science* **197,** 186–188 (1977).

45. Gorbunov, M. Y. & Falkowski, P. G. Photoreceptors in the cnidarian hosts allow symbiotic corals to sense blue moonlight. *Limnology and Oceanography* **47,** 309–315 (2002).

46. Langmead, B. & Salzberg, S. L. Fast gapped-read alignment with Bowtie 2. *Nat. Methods* **9,** 357–359 (2012).

47. Edgar, R. C. MUSCLE: multiple sequence alignment with high accuracy and high throughput. *Nucleic Acids Research* **32,** 1792–1797 (2004).

48. Galtier, N., Gouy, M. & Gautier, C. SeaView and Phylo_win, two graphic tools for sequence alignment and molecular phylogeny. *Comput Applic Biosci.* **12**, 543-548 (1996).

49. Fu, L., Niu, B., Zhu, Z., Wu, S. & Li, W. CD-HIT: accelerated for clustering the next-generation sequencing data. *Bioinformatics* **28,** 3150–3152 (2012).

50. Kumar, S., Stecher, G. & Tamura, K. MEGA7: Molecular Evolutionary Genetics Analysis Version 7.0 for Bigger Datasets. *Mol. Biol. and Evol.* **33,** 1870–1874 (2016).

51. Silvestro, D. & Michalak, I. raxmlGUI: a graphical front-end for RAxML. *Org. Divers Evol.* **12,** 335–337 (2012).

52. Ronquist, F. *et al.* MrBayes 3.2: efficient Bayesian phylogenetic inference and model choice across a large model space. *Systematic Biology* **61,** 539–542 (2012).

53. Leclère, L. & Rentzsch, F. Repeated evolution of identical domain architecture in metazoan netrin domain-containing proteins. *Genome Biology and Evolution*

**4,** 883–899 (2012).

54. Lapébie, P. *et al.* Differential responses to Wnt and PCP disruption predict expression and developmental function of conserved and novel genes in a cnidarian. *PLoS Genet* **10,** e1004590 (2014).

55. Sinigaglia, C., Thiel, D., Hejnol, A., Houliston, E. & Leclère, L. A safer, urea-based in situ hybridization method improves detection of gene expression in diverse animal species. (2017). doi:10.1101/133470

56. Hwang, W. Y. *et al.* Efficient genome editing in zebrafish using a CRISPR-Cas system. *Nat. Biotechnol.* **31,** 227–229 (2013).

57. Carré, D. & Carré, C. Origin of germ cells, sex determination, and sex inversion in medusae of the genus Clytia (Hydrozoa, leptomedusae): the influence of temperature. *J. Exp. Zool.* **287,** 233–242 (2000).

58. Brinkman, E. K., Chen, T., Amendola, M. & van Steensel, B. Easy quantitative assessment of genome editing by sequence trace decomposition. *Nucleic Acids Research* **42,** e168–e168 (2014).

59. Spitzer, M., Wildenhain, J., Rappsilber, J. & Tyers, M. BoxPlotR: a web tool for generation of box plots. *Nat. Methods* **11,** 121–122 (2014).

# Figures and Legends

## Figure 1. Spawning spectral characterisation of *Clytia* ovaries.

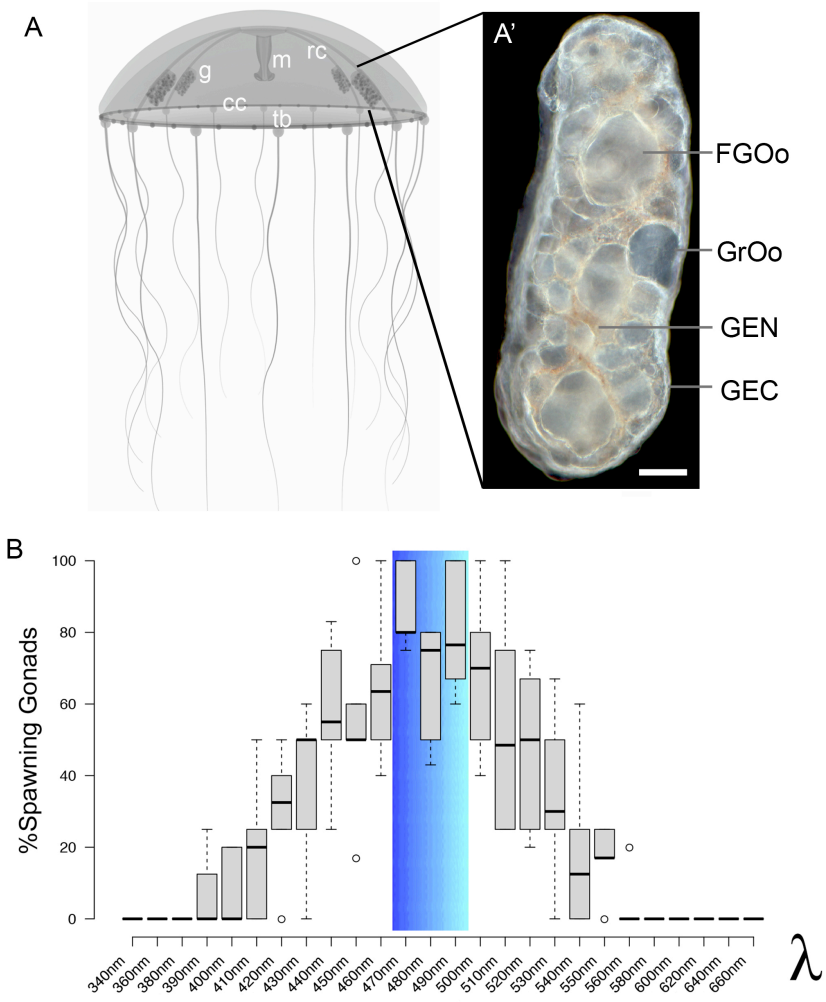


A) Schematic of a *Clytia hemisphaerica* female jellyfish: The four gonads (g) lie on the radial canals (rc) that connect the manubrium (M) to the circular canal (cc) running around the bell rim, adjacent to the tentacle bulbs (tb). A') Photo of a *Clytia* ovary. FGOo = fully-grown oocytes; GrOo = growing oocytes; GEN = gonad endoderm; GEC = gonad ectoderm. Bar = 100 µm. B) BoxPlot showing spectral characterisation of *Clytia* spawning. Groups of 3-6 isolated gonads were exposed to 10-second pulses of monochromatic light (see methods). Gonads were considered to spawn if at least one oocyte underwent maturation and release. Statistics were based on percentage of gonad spawning in response to a specific wavelength obtained from 5-6 independent experiments. A total of 20-30 gonads were analysed per wavelength. Centre lines show the medians; box limits indicate the 25th and 75th percentiles (1$^{st}$ and 3$^{rd}$ quartiles) as determined by R software; whiskers extend 1.5 times the interquartile

range from the 25th and 75th percentiles; outliers are represented by circles. Colour spectrum is shown only for wavelengths with medians of 75% or higher (470nm – 490nm). λ = wavelength.

**Figure 2. *Clytia Opsin* expression in gonad ectoderm cells**

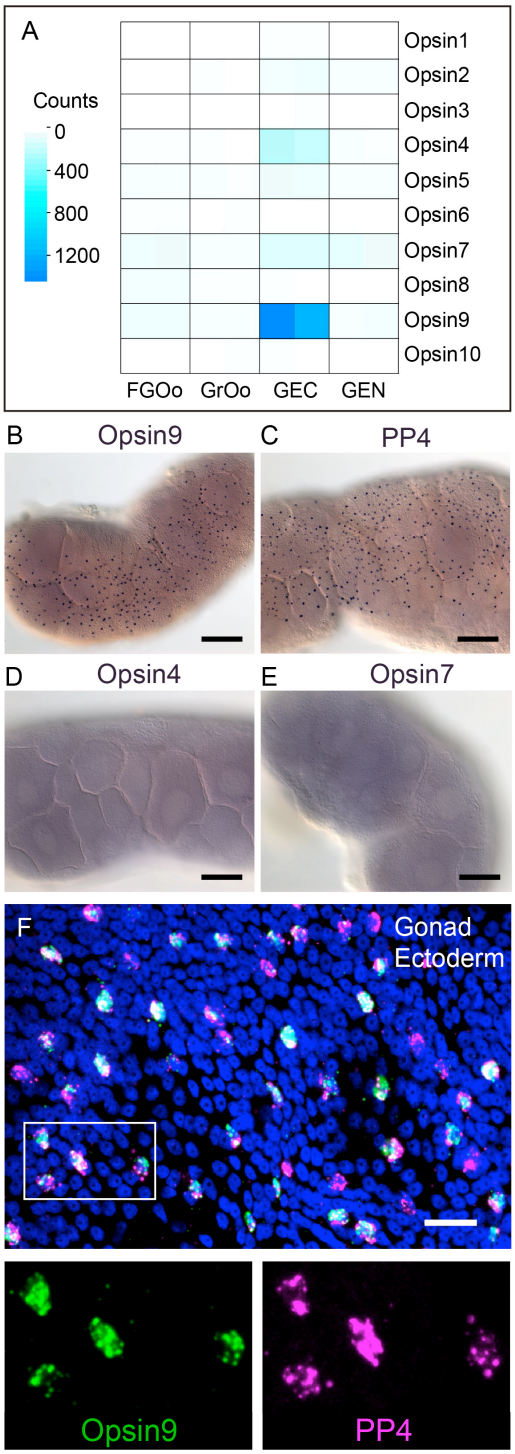


A) Heat map representing the expression of the ten opsin sequences from *Clytia hemisphaerica* in different gonad tissues. Illumina HiSeq 50nt reads from isolated endoderm (GEN), ectoderm (GEC), growing (GrOo) and fully-grown oocytes (FGOo) from mature female ovaries were mapped against the opsin sequences. Counts were normalised per total number of reads in each sample and per sequence length. B) *In situ* hybridisation (ISH) detection of *Opsin9* mRNA in scattered ectodermal cells of

female *Clytia* gonads. C) ISH of the neuropeptide precursor *PP4* mRNA in *Clytia* female gonads, also showing a scattered pattern in the ectoderm. D-E) ISH of *Opsin4* and *Opsin7* mRNAs, respectively, in *Clytia* ovaries, showing no detectable localised expression of these two opsin genes. F) Double fluorescent ISH showing co-expression of *Opsin9* (green) and *PP4* (magenta) mRNAs in gonad ectoderm cells; nuclei (Hoechst) in blue. Single channels are shown for the outlined zone in the top image. Of n = 594 randomly chosen cells expressing either gene counted in 10 different gonads, over 86% co-expressed Opsin9 and PP4 mRNAs. Controls with single probes were performed to validate a correct fluorescence inactivation and ensure that the two channels did not cross-react (not shown). Scale bars in B-E = 100 µm; F = 20 µm.

**Figure 3. Production and phenotype of *Opsin9* knock-out medusae.**

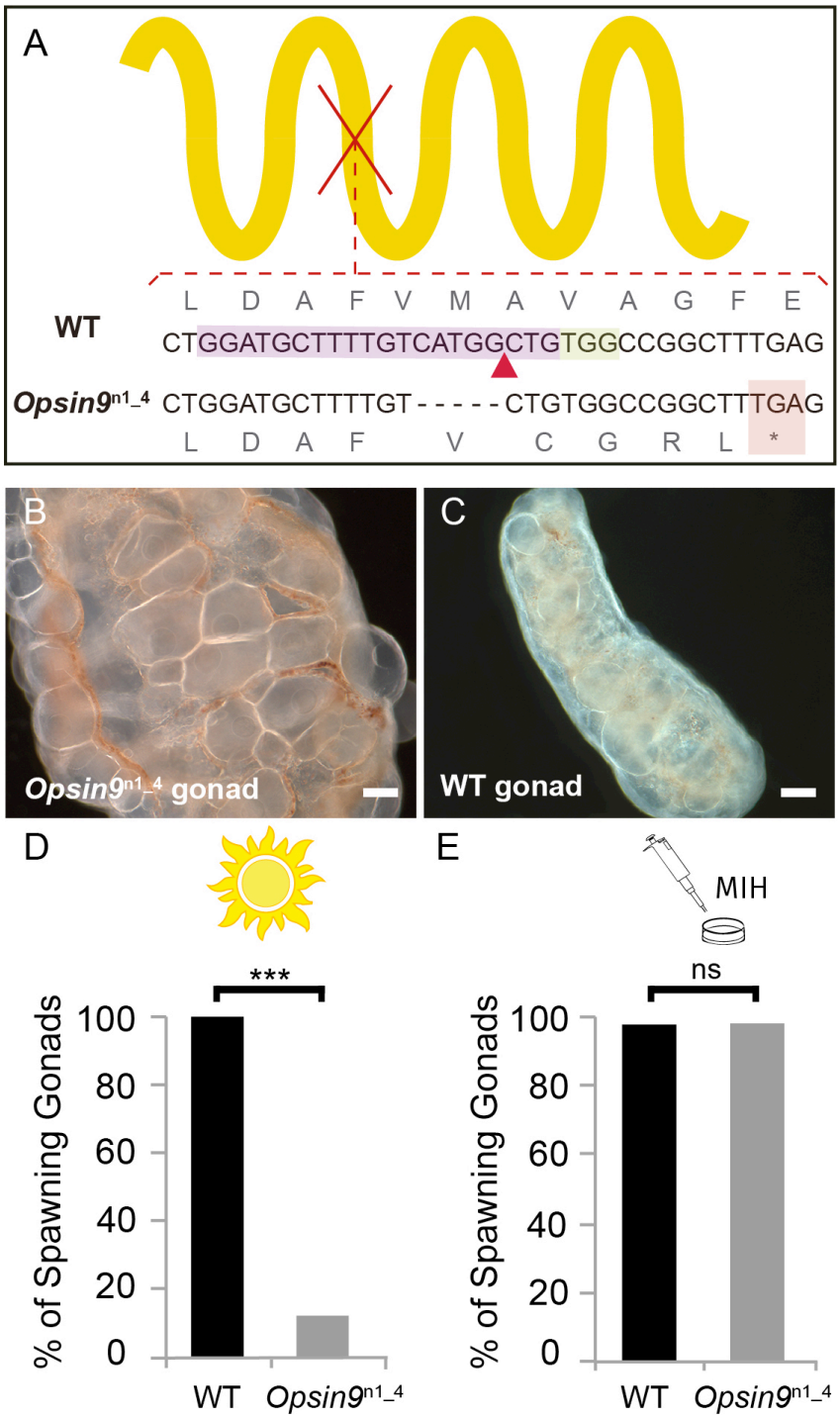


A) Scheme of Opsin9 GPCR showing part of the genomic region coding for the 3rd transmembrane domain targeted by *Opsin9* n1_4 CRISPR sgRNA. Corresponding amino acids are shown. Pink box indicates the target site of the sgRNA. Green box is the PAM sequence (NGG). The expected cleavage site of Cas9 is indicated by a red triangle. The predominant 5-bp deletion of *Opsin9*$^{n1\_4}$ is shown. This mutation leads

to a frame-shift and an early STOP codon in *Opsin9*$^{n1-4}$ (red box). B) Highly inflated gonad of an *Opsin9*$^{n1-4}$ mutant female jellyfish showing the abnormal accumulation of large oocytes. C) Wild type *Clytia* gonad at the same magnification. Images in B and C were both taken 8 hours after the natural light cue, accounting for the absence of fully grown oocytes in the wild type gonad. Scale bars all 100 µm. D) Quantification of spawning upon light stimulation of wild type (WT) and *Opsin9*$^{n1-4}$ gonads. Percentage of spawning gonads combined from 3 independent experiments is shown in all cases; n = 92 for wild type and n= 154 gonads for *Opsin9*$^{n1-4}$mutants. The Fisher exact test showed significant differences (F = 0) between wild types and mutants. E) Equivalent analysis for synthetic MIH treatment of wild type and *Opsin9*$^{n1-4}$ gonads. Oocyte maturation and spawning were rescued by synthetic MIH treatment; n = 94 gonads for wild type and n= 80 gonads for *Opsin9*$^{n1-4}$ mutants. Fisher exact test did not show significant differences (F = 0.595) between wild types and mutants.

**Figure 4. Accumulation of MIH in *Opsin9* mutant gonads.**

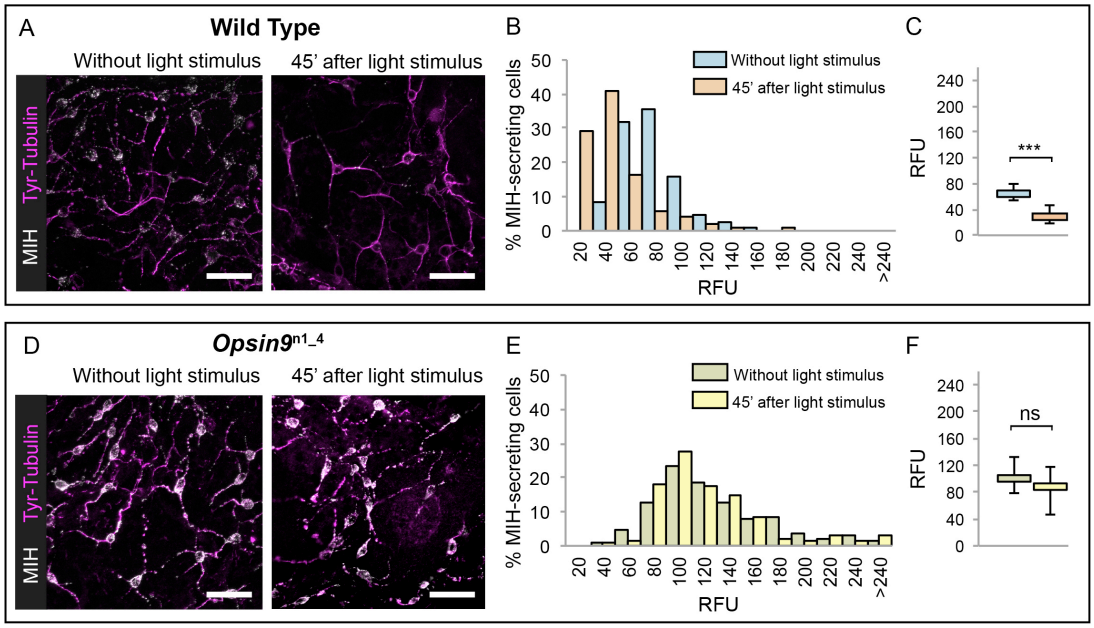


MIH content of ectoderm neural cells compared by quantitative imaging of the gonad surface of gonads fixed before and after light stimulation. All images were summed from 10 confocal Z planes over 4 µm, acquired on the same day using constant settings. Immunofluorescence using anti-PRPamide antibodies (MIH; white) was quantified in neural cells identified by typical morphology revealed by anti-tyrosinated tubulin (magenta) antibodies. A) Representative images of wild type *Clytia* gonad MIH-secreting cells showing reduction in MIH fluorescence after light stimulation. B) Distribution of RFU (Relative Fluorescence Units) values obtained for each neural cell analysed in the two conditions (number of cells analysed: n = 226 and n = 282, respectively). C) Graph showing the medians of the data in (B). Limits correspond to 1$^{st}$ and 3$^{rd}$ quartiles. The Mann-Whitney U test showed a significant difference between conditions ($p < 0.001$). D) Representative immunofluorescence images of *Opsin9*$^{n1–4}$ *Clytia* gonad MIH-secreting cells before and after light stimulation. MIH fluorescence is maintained upon light stimulation. E) Distribution of RFU values after fluorescence quantification in *Opsin9*$^{n1–4}$ MIH-secreting cells in the two conditions (n = 183 and n = 201, respectively). F) Graph showing the medians and quartiles of the data in (E). Mann-Whitney U test did not show a significant difference ($p = 0.976$). Scale bars all 20 µm.

**Figure 5. Morphology of *Clytia* MIH-secreting cells.**

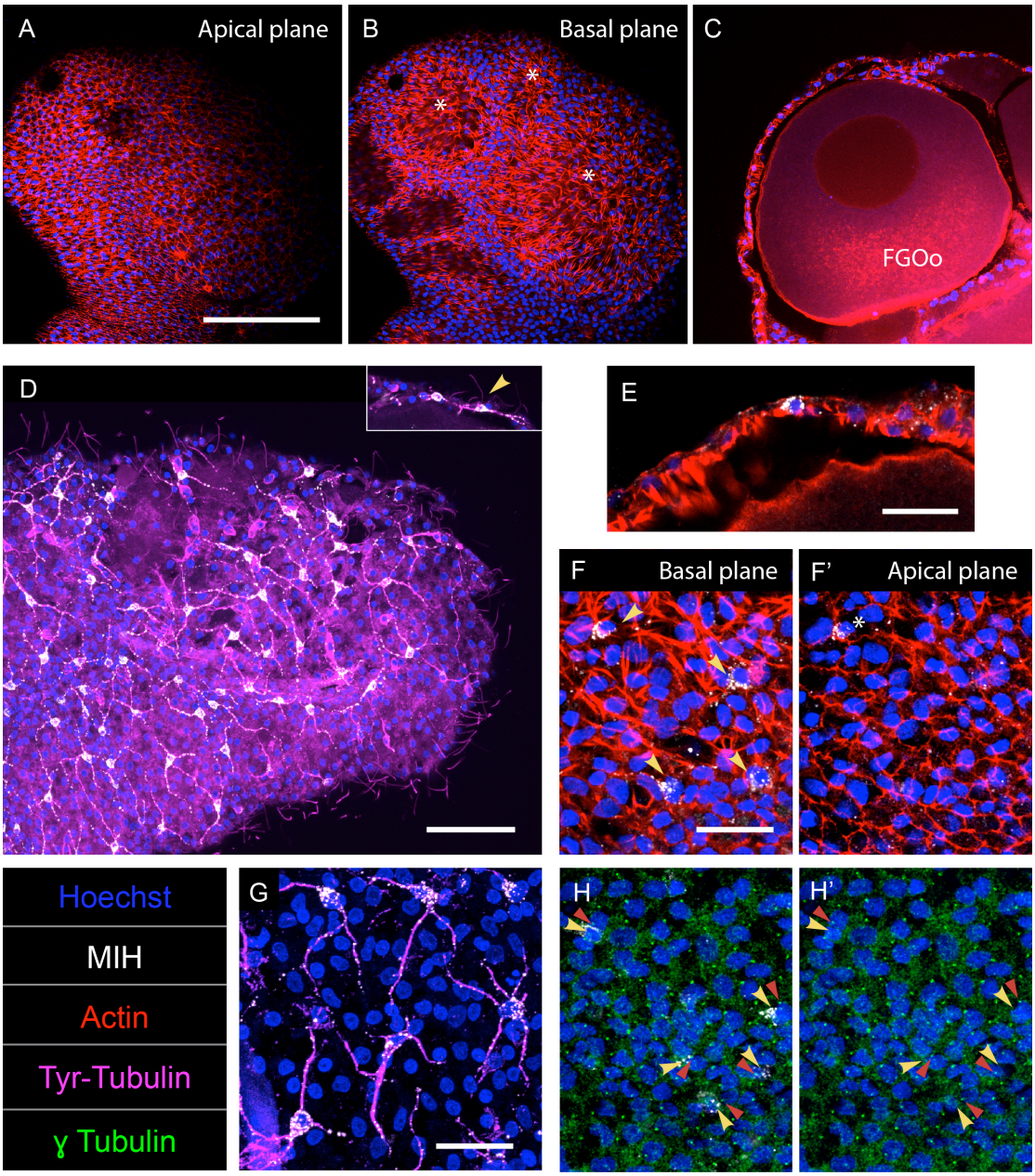


Immunofluorescence of *Clytia* ovaries with focus on the gonad ectoderm epitheliomuscular cells and MIH-secreting cells. Staining with Hoechst (blue), anti-PRPa (MIH - white), phalloidin (red), anti-tyrosinated tubulin (magenta), and anti-ɣ tubulin (green). A) Confocal plane taken at the gonad surface. Phalloidin decorates the apical junctions between epitheliomuscular cells. B) Same gonad as in (A) in a plane corresponding to the basal level of the ectoderm in areas overlying large oocytes (asterisks); phalloidin strongly stains the epitheliomuscular muscle fibres. C) Deeper Z plane from another gonad cutting through a fully-grown oocyte (FGOo) showing the monolayer of the thin gonad ectoderm and the relationship of the

epitheliomuscular fibres to the underlying oocytes. D) Confocal image of a gonad showing the distribution of MIH-secreting neural cells in the ectoderm (16 confocal Z planes were summed over 7µm depth at the gonad surface). Cilia were stained with anti-tyr-tubulin antibodies on epitheliomuscular cells, and could tentatively be detected on some MIH-secreting cells (Top right inset - yellow arrowhead). E) Higher magnification image of a MIH-secreting cell inserted in the myoepithelial layer. F, F') Two Z planes through the basal (F) and apical (F') planes of the epithelial layer. The cell bodies, nuclei and neural processes of the MIH-secreting cells (yellow arrowheads) are mainly in the basal plane, at the same level as the basal muscle fibres of the epitheliomuscular cells, however traces of MIH can be detected at the apical surface for some cells (asterisk). G) Higher magnification image of MIH-secreting cells showing the lack of obvious connections between neural processes. H, H') Gonad ectoderm surface Z plane showing ciliary basal bodies (stained for ɣ tubulin) of both epitheliomuscular cells and MIH-secreting cells (yellow arrowheads point to MIH-secreting cells and red arrowheads point to the basal bodies most probably associated with them - MIH staining shown only in H for clarity). Scale bars in A-C = 100 µm; D = 50 µm; E-H' = 20 µm.

**Figure 6. Model for Opsin9 function in *Clytia* oocyte maturation.**

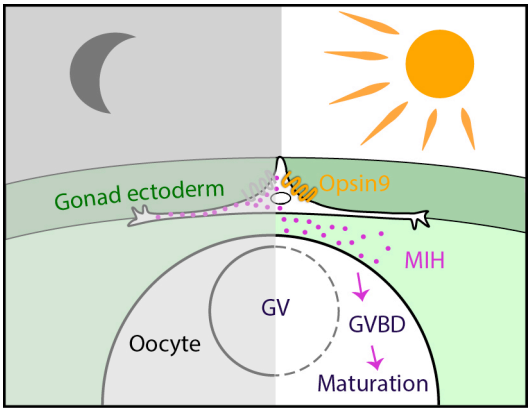


Model for *Clytia* oocyte maturation. At dawn, light activates Opsin9 in specialised neural cells of the gonad epithelium, causing secretion of MIH inside the gonad. MIH in turn acts on the oocyte surface to trigger the resumption of meiosis, followed by Germinal Vesicle breakdown (GVBD) and oocyte maturation.